Journal of Materials Chemistry C

Accepted Manuscript

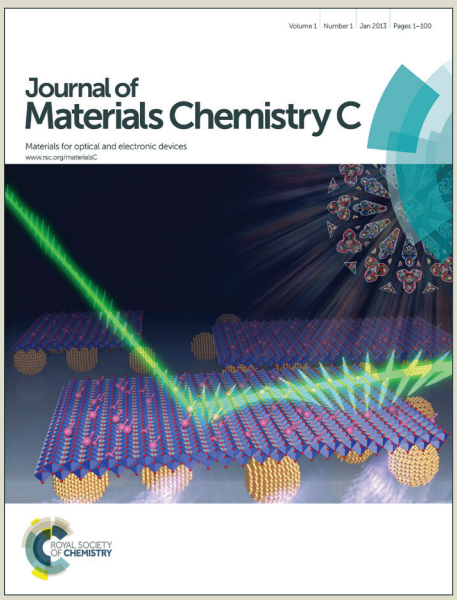

ROYAL SOCIETY OF CHEMISTRY

www.rsc.org/materialsC

Journal Name

RSCPublishing

ARTICLE

Exceptional Dielectric Performance Induced by the Stepwise Reversible Phase Transitions of an Organic Crystal: Betainium Chlorodifluoroacetate

Cite this: DOI: 10.1039/x0xx00000x

Zhihua Sun,[a,b,c] Shuquan Zhang,[a,b] Chengmin Ji,[a] Tianliang Chen,[a] Junhua Luo [*a, b]

Received 00th January 2014,
Accepted 00th January 2014

DOI: 10.1039/x0xx00000x

www.rsc.org/

Solid-state phase transition materials with the electric ordering are of great interest owing to their technological importance. In the present work, a new molecular co-crystal material, betainium chlorodifluoroacetate (**1**) was synthesized, which exhibits exceptional dielectric performance, originating from the distinct structural changes and phase transitions induced by the stepwise orderings of chlorodifluoroacetate anions. Measurements of its temperature-dependent dielectric constant show the pronounced and successive anomalies at 131 (T_c), 178 (T_2) and 220 K (T_3), respectively. Such dielectric orderings are coincident with a series of reversible thermal peaks in DSC and specific heat curves. Moreover, a large heat hysteresis of ~15 K at T_c indicates that **1** undergoes a first-order reversible phase transition with the symmetry transformation from $P2_1/m$ to $P2_1/c$, which is further confirmed by the structure analyses. For the origin of its pronounced dielectric response, the totally frozen ordering and reorientation of anionic parts are found to dominate its structural change at T_c (*i.e.* the order-disorder transformation), while the other two dielectric anomalies at 178 and 220 K are merely involved with partial ordering of CF_2ClCOO^- moieties. The investigation will afford a broader design flexibility and may thus facilitate the development of molecular functional materials.

Introduction

Dielectric phase transition materials have attracted intensive interest owing to their potential applications as the fundamental components of modern electrical and electronic devices,[1] which are based on their diverse dielectric responses such as the high dielectric constants, dielectric tunability and dispersion, *etc*.[2] Engineering of solid-state materials with distinctive dielectric behaviors is crucial not only for the exploration of novel physical properties, but also for the theoretical study of the structure-property relationship.[3] Thus, various approaches have been developed and one of the most efficient strategies is to introduce the dynamic moieties that are sensitive to the temperature change, which can induce the structural phase transition coupling with potential dielectric responses.[4] In the close-packed molecular ionic or co-crystal system, the moieties with small volume and high intramolecular symmetry are eligible for reorientation due to their lower energy barrier. For example, the order-disorder changes of diisopropylammonium cation are found to trigger the ferroelectric phase transition with high dielectric constants and low dielectric loss.[5] In addition, orderings of partial halogen atoms in the haloacetate anions, such as CF_3COO^-, CCl_2HCOO^- and CCl_3COO^-, have also been observed to dominate the dielectric phase transitions in the molecular switchable dielectric materials.[6] In the case of nonlinear optical switching material, $[Hdabco]^+[CF_3COO]^-$, the slowing down of trifluoromethyl group results in its structure change, corresponding to the remarkable dielectric response.[7] Such studies of compounds composed by haloacetate components reveal that they have the potential to undertake a key role in constructing new phase transition materials with the attractive dielectric performance, owing to their striking features of order-disorder transformation.

Betaine is the trimethyl-glycine with a zwitter-ion structure,[8] which has been used to assemble the ferroic materials, such as betainium phosphate,[9] betainium phosphite [10] and betainium arsenate, *etc*.[11] The crystals of this family are found to show a large variety of phase transitions including ferroelectric, antiferroelectric and antiferrodistortive ones, *etc*. Moreover, they also exhibit the

incommensurate phases and glass behaviors during phase transitions.[8-11] In this context, betaine would be a good candidate molecule to construct the dielectric phase transition materials with other inorganic or organic acids. Here, we report the successive dielectric anomalies at 131 (T_c), 178 and 220 K of an organic molecular co-crystal, betainium chlorodifluoroacetate (**1**, see scheme 1), which originate from its structural changes and phase transitions induced by stepwise orderings of chlorodifluoroacetate anions. Variable-temperature X-ray structure determination, thermal analyses including differential scanning calorimetry (DSC) and specific heat were carried out to confirm its phase transitions.

Experimental Section

Compound **1** was synthesized from the solution (containing 1:1 of water and ethanol) with the equimolar chlorodifluoroacetic acid and betaine. Colorless plate-like crystals were easily obtained after a few days. Its deuterated compound was obtained by the re-crystallization of **1** for several times from the D_2O solutions. The phase purity is confirmed by its powder XRD, which matches well with its room-temperature structure determination (Figures S1-S2). The formation of hydrogen-bonded binary compound is verified by IR spectra, in which several vibrations around 1730 cm^{-1} (ν_{COOH}) and 2969 cm^{-1} (ν_{OH}) are distinct from that of the zwitterionic betaine.

Variable-temperature X-ray single-crystal diffraction data of **1** were collected using a Super Nova CCD diffractometer with the graphite monochromated Mo-$K\alpha$ radiation (λ = 0.71073 Å) at different temperatures. Colorless crystals of approximate dimensions 0.46 × 0.37 × 0.28 mm^3 were used in the data collection. The CrystalClear software package (Rigaku) was used for data collection, cell refinement and data reduction. Crystal structures were solved by the direct methods and refined by the full-matrix least-squares method based on F^2 using the SHELXLTL software package. All non-hydrogen atoms were refined anisotropically and the positions of hydrogen atoms were generated geometrically. Crystallographic data and details of data collection and refinement are listed in Table 1, and CCDC 1016861-1016864 contain the supplementary crystallographic data for this paper.

DSC and specific heat measurements of **1** were carried out on NETZCSCH DSC 200 F3 instrument by heating and cooling rate of 5 K/min in the temperature range from 100 to 250 K. All the measurements were performed under the nitrogen atmosphere in the aluminum crucibles. In the dielectric experiments, the powder sample and single-crystal plate of **1** with silver pasted as electrodes were used for measuring the complex dielectric permittivities, $\varepsilon = \varepsilon' - i\varepsilon''$, using a TH2828A impedance analyzer at the respective frequencies with the AC voltage of 1 V.

Results and discussion

As an effective method to probe whether the compound undergoes temperature-induced structural phase transition, DSC measurements were performed on the polycrystalline samples of **1**. It is noteworthy that a sharp endothermic peak at 134 K (T_c) upon heating is clearly observed, together with a main exothermic peak at 119 K in the cooling mode (Figure 1a). The sharp pattern of these two reversible peaks and large thermal hysteresis of ~15 K disclose that **1** undergo a first-order phase transition at T_c. Interestingly, two pairs of tenuous thermal peaks are also recorded in both cooling and heating modes. One endothermic peak is at 178 (T_2) and the other is located at 220 K (T_3) in the warming mode, respectively. These reversible heat anomalies may probably be involved with the partial orderings of moieties in **1**, which needs further investigation. In addition, the experimental results of specific heat carried out on a crystal piece of **1** present an extremely sharp peak at ~134 K, similar to that of KDP,[12] which strongly supports that the phase transition of **1** belongs to the first-order type at T_c. As expected, other thermal anomalies are also observed in the C_p-T trace, which correspond well to the DSC results.

The entropy change (ΔS) of the structural phase transition at T_c is estimated from the heat capacity data to be ~13.16 J K^{-1} mol^{-1}. According to the Boltzmann equation, $\Delta S = R \ln N$, where N denotes the ratio of possible configurations and R is the gas constant, it is found that N = 4.9, revealing the order-disorder feature of the phase transition.[13] Such a large configuration value (much greater than 2) also suggests a high degree of disorder in the crystal structure of **1**, which originates from the dynamical disordering of chlorodifluoroacetate groups in the state above T_c (see the following structure analyses).

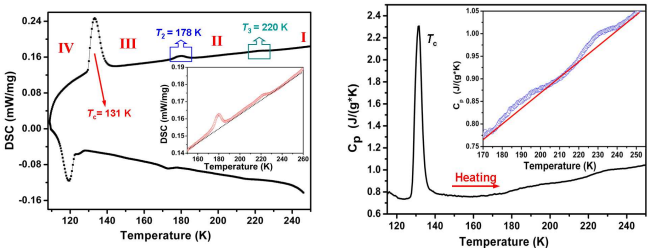

(a) (b)

Figure 1. (a) DSC curves of **1**. Insert presents detectable thermal anomalies at T_2 and T_3. (b) Temperature dependence of specific heat of **1** obtained in the warming mode with the rate of 5 K/min. Insert also reveal thermal anomalies at T_2 and T_3, which agree well with the DSC results.

To further investigate the structural phase transition of **1**, its crystal structures were determined at different temperatures. Table 1 gives the cell parameters and refinement detail. For convenience, we label the four different states as I, II, III and IV, respectively (Figure 1a). Actually, **1** always crystallizes in the monoclinic crystal system with the same space group of $P2_1/m$ in the states of I, II and III. The cell parameters display no obvious changes, which can be described

as the high-temperature phase (HTP, above T_c). Below T_c, its crystal structure was solved by the monoclinic space group of $P2_1/c$, and the cell parameters demonstrate evident changes, such as the doubling of its *c*-axis length and cell volume. Although such a change of two related phases does not follow the group-subgroup relationship based on Curie symmetry principle, the determination of $P2_1/c$ gives the finally acceptable refinement converged to $R_1/wR_2 = 0.0517/0.1070$. Probably, the crystallographic symmetry of **1** may be even lower; however, the absence of second-order nonlinear optical activities suggests that **1** should at least crystallize in the centrosymmetric space group. In addition, the value of β angle also shows an obvious change (from about 94.5° to 97.1°). For such dramatic changes of the cell parameters, the feature of its phase transition can be ascertained by measuring unit cell parameters as a function of temperature. The results show that cell parameters of *c*-axis, β-angle and volume exhibit abrupt change at T_c (Figure S4), which discloses its characters of first-order phase transition, in fairly good agreement with thermal analyses. However, cell parameters of **1** show no obvious changes around T_2 and T_3, suggesting that the driving forces of these reversible thermal entropy were too weak to trigger the change of its cell parameters.[14] These results of the cell parameters variation would further illuminate that the reversible heat anomalies at 178 and 220 K may probably be involved with the partial orderings of CF_2ClCOO^- moieties in **1**.

For convenience, molecular structures of **1** collected at 230 K and 100 K were determined as the representative modes for its HTP and LTP, respectively (Figure 2). In HTP, the chlorodifluoroacetate moiety is located in the disordered state with F atoms being split (0.64:0.36), which are thus in the satisfaction of its crystallographic symmetry. It is noteworthy that a mirror plane is depicted, lying on the atoms of cation (C4, N1, C2, C1 and O1), and atoms of the anion (C5, C6, Cl1 and F1), corresponding well to its mirror symmetry *m*(*x*, 1/4, *z*). The highly-symmetric O-H···O hydrogen bonds of weak interactions (with the O···O distance of 2.977 Å) can be found between the anions and betainium cations, forming the H-bonded dimers. The observation of H-bonding interactions is also coincident with such a high operating symmetry of the mirror plane, as shown in Figure 2a.

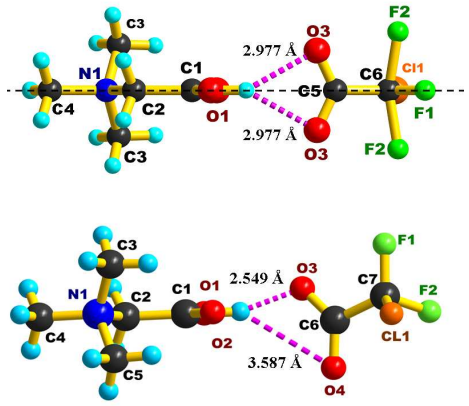

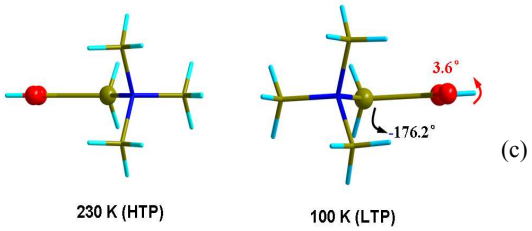

Figure 2. Molecular structures of **1** collected at 230 K (a) and 100 K (b), as the representative models for its HTP and LTP, respectively. The dotted pink lines indicate intermolecular O-H···O H-bonding interactions. (c) Molecular configuration of the betainium cation shows an attritive small-angle torsion in LTP.

Although **1** undergoes the successive thermal anomalies, it appears that the disordering of its anionic moiety takes place over a very wide temperature range (from room temperature down to 134 K, see Table 1), which de-emphasizes the order-disorder feature of its transition. Crystal structures determined at 230, 200 and 150 K were always located at the similar disordering, except for the variations of atomic thermal ellipsoids. In detail, thermal ellipsoids of anions, particularly for F atoms, are much larger than those of other atoms in **1** (Figure S6). For instance, average values of the orthogonalized U_{ij} tensor for F atoms are about three times larger than other atoms. During its successive transitions, the ratios of U_{eq} (average of F atoms)/U_{eq} (N atom in cation) at different temperatures were estimated as $150.5/34^{230K}$, $136.5/31^{200K}$, $105/25^{150K}$ and $37/20^{100K}$, respectively. Obviously, the slight diminution for nitrogen atom results from its cooling contraction; while the gradual variation for F atoms is caused by the atomic orderings. These results further disclose its typical disorder-order feature. When the temperature decreases below T_c (in LTP), the disordered chlorodifluoroacetate anions of **1** are eventually frozen into ordering with all the atoms being determined at their exclusive sites (Figure 2b). During this process, the mirror plane of its molecular dimer disappears, owing to the reorientation of CF_2ClCOO^- moiety. The loss of this plane can also be deduced from the molecular configuration of betainium cations. In HTP, the torsion angles of C_1-C_2-N_1-C_4 and O_1-C_1-C_2-N_1 are calculated as -180° and 0°, which strongly support the presence of the symmetric plane. However, these values become to be -176.2° and 3.6° in LTP, revealing that the betainium cation undergoes a small-angle twisting motion (Figure 2c). The driving force for this motion is thought to come from thermal vibrations of the chain-like skeleton around the equilibrium positions. When temperature lowers below T_c, thermal-induced motion of skeleton is restricted, showing the deviation from its symmetry plane. Moreover, the asymmetric O-H···O hydrogen bonds (with O···O distances of 2.549 and 3.587 Å) are caused by the reorientation of CF_2ClCOO^- moiety. In LTP, the carboxyl group seems to fall down while halogenated methyl part moves upwards, leading to the disappearance of mirror plane. Such a symmetry transformation agrees fairly with the change of its spatial symmetric operations as shown in Figure 3.

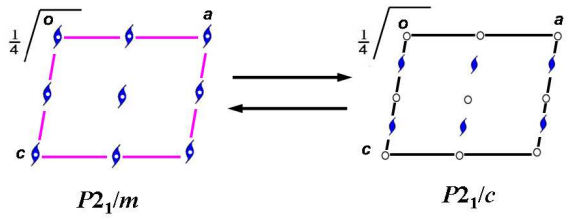

Figure 3. Symmetry transformation of **1** from space group of $P2_1/m$ (HTP) to $P2_1/c$ (LTP). The symmetry operations change from 1; 2(0,0,1/2) 0,0, z; ī (0,0,0) and *m* (*x*, *y*, 1/4) to 1; 2(0,0,1/2) 1/4,2, z; ī (0,0,0) and *a* (*x*, *y*, 1/4). The delicate changes of site symmetry are involved with its structure variations.

Variable-temperature dielectric measurements are not only sensitive to the temperature-induced phase transition or structure changes, but also essential for dielectric materials in practical device application. Measurements of the complex dielectric permittivities ($\varepsilon = \varepsilon' - i\varepsilon''$) of **1** were performed on both powder and single-crystal samples in the heating mode. Figure 4 presents the real parts (ε') of its complex dielectric permittivities and the corresponding imaginary parts (ε'') as a function of temperature. It is clearly shown that three "peak-like" dielectric anomalies are recorded in the temperature range from 100 to 240 K, which corresponds well to DSC and specific heat results, suggesting its successive phase transitions. Emphatically, both the ε' and ε'' results display more abrupt jump with an obvious enhancement at T_c, while the changes at T_2 and T_3 are slightly peaceful. Such an amplitude difference of dielectric performance suggests that the structure variation of **1** is much more drastic at T_c; that is, phase transition induced by the total frozen ordering affords the more plenteous driving forces, in contrast with structure changes involved with the partial orderings at T_2 and T_3, which coincides well with the crystal structure analyses.

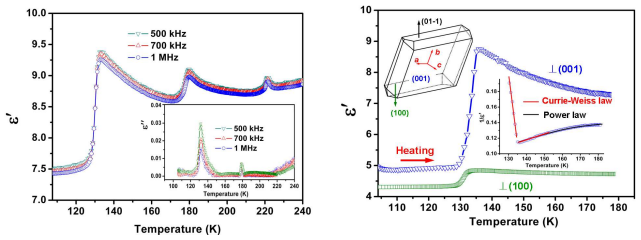

(a) (b)

Figure 4. (a) Temperature-dependence of the complex dielectric permittivities of **1** measured on the powder sample under different frequencies. Both the real parts and imaginary parts present much more abrupt changes at T_c than other two temperature points. (b) The real parts versus temperature measured on crystal samples with the different crystallographic directions (f = 1 MHz).

Since the patterns of $\varepsilon'(T)$ in Figure 4a is similar to that of copper-formate tetrahydrate (an antiferroelectric material) at T_c,[15] which provides the indicative information if the disorder is dynamic or static, dielectric measurements were performed on single crystals of **1** along different crystallographic directions from 100 to 180 K. During the phase transition, $\varepsilon'(T)$ follows the Curie-Weiss law $1/\varepsilon' = (T - T_0)/C$ in the vicinity of T_c (the insert in Figure 4b),[16] giving the values T_0 = 128 K ($T_0 < T_c$) and $C \approx 65$. Such results suggest that **1** should undergo a first-order phase transition. Actually, the other power law, such as $1/\varepsilon' = A + C_2^{-k}(T - T_2)^k$ may also be used to describe the temperature-dependent dielectric activities of **1** in an even wider temperature range above T_c. resembling that of betainium phosphate.[9] The estimated value of k is ~1.085 (with A = 0.065 and C_2 = 491), which is slightly different from the value from the Curie-Weiss law (k = 1).

Another striking feature of the results in Figure 4b is that it presents a high anisotropy of dielectric response at phase transition point; namely, the (001) plate gives a larger varying change than that of (100) plate. In detail, values of dielectric constant perpendicular to the (001) plate show a change of $\Delta\varepsilon_c' = 4.9$, while a smaller anomaly of $\Delta\varepsilon_a' \approx 0.6$ was clearly observed along its *a*-axis direction, thus confirming the dielectric anisotropy with $\Delta\varepsilon_c'/\Delta\varepsilon_a' \approx 8.2$. Here, such an anisotropy might be expected from the predominantive layer structure of this crystal, or the multiplication of its *c*-axis during the phase transition. As shown in Figure 5, during the dielectric phase transition, unit cell of **1** in LTP is twice as much as that in HTP with the elongation of *c*-axis length; while the other two crystallographic axes keep stable. Such an obvious difference of axis-length changes might account for the high anisotropy of its bulk dielectric response. Emphatically, although the betainium cation exhibits a quite small angle twisting motion, it should be also indispensable for the phase transition and the dielectric response of **1**. During the temperature cooling down, it behaves as the "stator-like" part to stabilize the H-bonding dimer and then leaves enough room for the potential reorientation of the chlorodifluoroacetate moiety. When the anions reorientate upwards or downwards away from the mirror plane, the main framwork of **1** keeps almost stable. In this context, the chlorodifluoroacetate anion and betainium cation of **1** match each other very well to trigger its dielectric phase transitions. Thus, it is probably deduced that the cooperation of fully frozen ordering (*i.e.* the order-disorder transformation) and the reorientation that leads to the structure change of **1** at T_c, as well as abrupt dielectric behaviors.

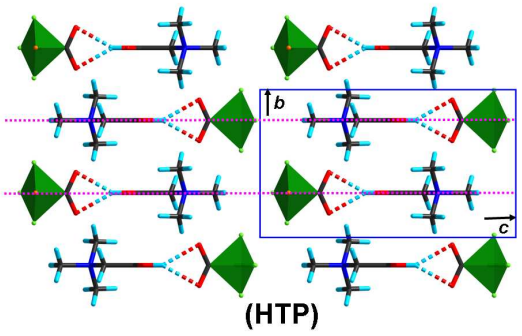

(a)

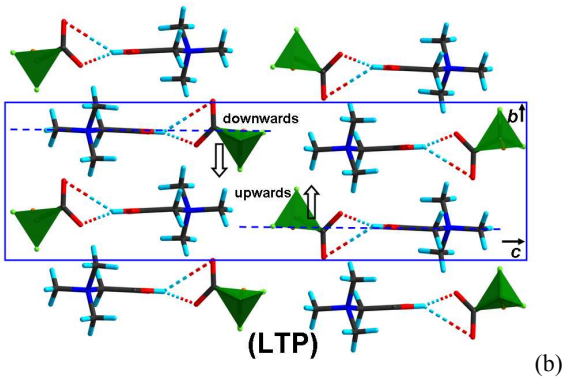

(b)

Figure 5. Crystal packing views of **1** along the *a*-axis direction in its HTP (a) and LTP (b). The disappearance of its mirror symmetry *m*(x, 1/4, z) is vividly displayed owing to the ordering and reorientation of chlorodifluoroacetate anions, and the *c*-axis shows the multiplication of length which may account for its pronounced dielectric anomalies.

For compound **1**, the O-H···O hydrogen bonding interactions connect its components closely and seem to be also involved with the structural phase transition, as shown in Figure 5. It is well-known that the substitution of deuterium for hydrogen would result in significant changes of physical properties in some hydrogen-bonded phase transition materials, such as the sharp enhancement of T_c and the obvious changes of dielectric constants, such as KH_2PO_4 and KD_2PO_4.[17] Here, the deuterated analogue of **1** was synthesized to examine its possible deuterium isotope effect.[18] It is notable that the polycrystalline powder of its deuterated analogue shows the similar thermal behaviors as **1** without any obvious isotope effects on T_c (see Figure S7), which would probably exclude the role of proton dynamics.[20] Such an evidence further confirms that its exceptional dielectric performance during phase transitions is triggered by the order-disorder transformation of the chlorodifluoroacetate anion of **1**.

Conclusion

In summary, the present work has demonstrated the striking dielectric performance in a new co-crystal material, betainium chlorodifluoroacetate. Its dielectric responses show pronounced peak-shape anomalies at 131, 178 and 220 K, which are strongly involved with the successive structural changes or phase transitions induced by the gradual orderings of chlorodifluoroacetate anions. Structure analyses reveal that it undergoes a first-order reversible phase transition at 131 K. The totally frozen ordering and reorientation of chlorodifluoroacetate anions are predominant during its structure phase transition. For the other two dielectric anomalies, it is found that the partial orderings of CF_2ClCOO^- moieties afford the driving force. Such dielectric activities induced by the stepwise order-disorder transformation discriminate from other previously reported dielectric materials, which may provide a potential platform for designing the new organic electric functional materials.

Acknowledgements

This work was financially supported by the National Nature Science Foundation of China (21222102, 21373220, 51102231, 21171166 and 21301171), the One Hundred Talents Program of the Chinese Academy of Sciences, the 973 Key Programs of the MOST (2010CB933501, 2011CB935904) and Key Project of Fujian Province (2012H0045) and Science Foundation for Distinguished Youth of Fujian Province (2014J06015). Dr. Sun thanks the support from "Chunmiao Project" of Haixi Institute of Chinese Academy of Sciences (CMZX-2013-002).

Notes and references

[a]Key Laboratory of Optoelectronic Materials Chemistry and Physics, Fujian Institute of Research on the Structure of Matter, Chinese Academy of Sciences, Fuzhou, Fujian，350002, P.R. China.
[b]State Key Laboratory of Structural Chemistry, Fujian Institute of Research on the Structure of Matter, Chinese Academy of Sciences, Fuzhou, Fujian，350002, P.R. China.
[c]State Key Laboratory of Crystal Materials, Shandong University, Jinan, 250100, China.
Corresponding E-mail: jhluo@fjirsm.ac.cn.

†Electronic supplementary information (ESI) available: X-ray crystallographic information files of **1** at different temperatures (100, 150, 200 and 230 K), PXRD patterns, Figures S1-S7.

1 (a) J. C. Burfoot and G. W. Taylor, *Polar Dielectrics and Their Applications*, University of California Press, California, **1979**; (b) M. Halik, H. Klauk, U. Zschieschang, G. Schmid, C. Dehm, M. Schütz, S. Maisch, F. Effenberger, M. Brunnbauer and F. Stellacci, *Nature*, 2004, **431**, 963; (c) P. Simon and Y. Gogotsi, *Nat. Mater*., 2008, **7**, 845.

2 (a) Q. M. Zhang, H. Li, M. Poh, F. Xia, Z.-Y. Cheng, H. Xu and C. Huang, *Nature*, 2002, **419**, 284; (b) Q. Ye, Y.-M. Song, G.-X. Wang, K. Chen, D.-W. Fu, P. W. Chan, J.-S. Zhu, S. D. Huang and R.-G. Xiong, *J. Am. Chem. Soc.* 2006, **128**, 6554; (c) S. Zhong, S. P. Alpay and J. V. Mantese, *Appl. Phys. Lett.* 2006, **88**, 132904; (d) C. H. Li, X. Q. Zhang, Z. Cheng and Y. Sun, *Appl. Phys. Lett*. 2008, **92**, 182903; (e) K.H. Mahmoud, F. M. Abdel-Rahim, K. Atef and Y.B. Saddeek, *Current Appl. Phys*. 2011, **11**, 55.

3 (a) J.-Z. Ge, X.-Q. Fu, T. Hang, Q. Ye and R.-G. Xiong, *Cryst. Growth Des*. 2010, **10**, 3632; (b) Z. Sun, J. Luo, T. Chen, L. Li, R.-G. Xiong, M.-L. Tong and M.. Hong, *Adv. Funct. Mater*. 2012, **22**, 4855; (c) Z. Sun, X. Wang, J. Luo, S. Zhang, D. Yuan and M. Hong, *J. Mater. Chem. C* 2013, **1**, 2561; (d) X. Shi, J. Luo, Z. Sun, S. Li, C. Ji, L. Li, L. Han, S. Zhang, D. Yuan and M. Hong, *Cryst. Growth Des*. 2013, **13**, 2081; (e) Y. Zhang, W.-Q. Liao, H.-Y. Ye, D.-W. Fu and R.-G. Xiong, *Cryst. Growth Des*. 2013, **13**, 4025; (f) Z. Sun, T. Chen, J. Luo, and M. Hong, *Angew. Chem. Int. Ed*. 2012, **51**, 3871.

4 (a) W. Zhang, Y. Cai, R.-G.Xiong, H. Yoshikawa and K. Awaga, *Angew. Chem. Int. Ed*. 2010, **49**, 6608; (b) W. Zhang, H.-Y. Ye, R. Graf, H. W. Spiess, Y.-F. Yao, R.-Q. Zhu and R.-G. Xiong, *J. Am. Chem. Soc.* 2013, **135**, 5230; (c) Q.-C. Zhang, F.-T. Wu, H.-M. Hao, H. Xu, H.-X. Zhao, L.-S. Long, R.-B. Huang and L.-S. Zheng, *Angew. Chem. Int. Ed*. 2013, **52**, 12602; (d) A. Katrusiak, M. Szafranski and G. J. McIntyre, *Phys. Rev. Lett*. 2002, **89**, 215507.

5 (a) D.-W. Fu, W. Zhang, H.-L. Cai , J.-Z. Ge, Y. Zhang and R.-G. Xiong, *Adv. Mater*. 2011, **23**, 5658; (b) D.-W. Fu, H.-L. Cai, Y. Liu, Q. Ye, W. Zhang, Y. Zhang, X.-Y. Chen, G. Giovannetti, M. Capone, J. Li and R.-G. Xiong, *Science* 2013, **339**, 425.

6 (a) M. Hashimoto, K. Hamada and K. Mano, *Bull. Chem. Soc. Jpn.* 1987, **60**, 1924; (b) M. Zdanowska-Fraczek, S. Lewicki, R. Jakubas and J. Wasicki, *Solid State Nuclear Magnetic Resonance*, 2000, **16**, 161; (c) M. Kunitomo, R. Etoh, T. Hayashi, T. Kohmoto, Y. Fukuda and T. Hashimoto, *J. Phys. Soc. Jpn.* 2002,

71, 955; (d) K. Saito, Y. Yamamura, N. Kikuchi, A. Nakao, S. Yasuzuka, Y. Akishige and Y. Murakami, *CrystEngComm*, 2011, **13**, 2693; (e) C. Ji, Z. Sun, S.-Q. Zhang, T. Chen, P. Zhou, Y. Tang, S. Zhao and J. Luo, *J. Mater. Chem. C*, 2014, **2**, 6134; (f) S. Li, J. Luo, Z. Sun, S. Zhang, L. Li, X. Shi and M. Hong, *Cryst. Growth Des.*, 2013, **13**, 2675.

7 Z. Sun, J. Luo, S. Zhang, C. Ji, L. Zhou, S. Li, F. Deng and M. Hong, *Adv. Mater.* 2013, **25**, 4159.

8 (a) M. Nakagawa, Y. Inomata and F. S. Howell, *Inorg. Chim. Acta*, 1999, **295**, 121; (b) C. Gabriel, E. Kioseoglou, J. Venetis, V. Psycharis, C. P. Raptopoulou, A. Terzis, G. Voyiatzis, M. Bertmer, C. Mateescu and A. Salifoglou, *Inorg. Chem.* 2012, **51**, 6056.

9 (a) J. Albers, A. Klöpperpiepe, H. J. Rother and K. H. Ehses, *Phys. Stat. Sol. (a)* 1982, **74**, 553; (b) S. L. Hutton, I. Fehst, R. Böhmer, M. Braune, B. Mertz, P. Lunkenheimer and A. Loidl, *Phys. Rev. Lett*. 1991, **66**, 1990; (c) J. Banys, S. Lapinskas, A. Kajokas, A. Matulis, C. Klimm, G. Völkel and A. Klöpperpieper, *Phys. Rev. B* 2002, **66**, 144113.

10 (a) I. Fehst, M. Paasch, S. L. Hutton, M. Braune, R. Böhmer, A. Loidl, M. Dörfel, Th. Narz, S. Haussühl and G. J. McIntyre, *Ferroelectrics* 1993, **138**, 1; (b) J. Banys, J. Macutkevic, C. Klimm, G. Völkel, A. Kajokas, A. Brilingas and J. Grigas, *Phys. Status Solidi A* **2004**, *201*, 602; (c) E. V. Balashova, B. B. Krichevtsov and V. V. Lemanov, *J. Appl. Phys*. 2008, **104**, 126104.

11 (a) A. Klöpperpieper, H.J. Rother, J. Albers and K. H. Ehses, *Ferroelectrics Lett.* 1982, **44**, 115; (b) J. Albers, A. Klöpperpieper, H. E. Müser and H.J. Rother, *Ferroelectrics* 1984, **54**, 45; (c) H.J. Rother, J. Albers, A. Klöpperpieper and H. E. Müser, *Jpn. J. Appl. Phys*. 1985, **24**, 384.

12 (a) P. G. Gennes, *Solid State Comm*. 1963, **1**, 132; (b) P. S. Peercy, *Phy. Rev. B* 1975, **12**, 2725; (c) P. Tomaszewski, *Phase Transitions* 1992, **38**, 127; (d) A. Katrusiak, *Phys. Rev. B* 1993, **48**, 2992.

13 Y. Zhang, H.-Y. Ye, H.-L. Cai, D.-W. Fu, Q. Ye, W. Zhang, Q. Zhou, Jinlan Wang , G.-L. Yuan and R.-G. Xiong, *Adv. Mater*. 2014, **26**, 4515.

14 Y. Zhang, W.-Q. Liao, H.-Y.Ye, D.-W. Fu and R.-G. Xiong, *Cryst. Growth Des*. 2013, **13**, 4025.

15 (a) K. Okada, *Phys. Rev. Lett*. 1965, **15**, 252; b) K. Okada, *Phys. Rev.* 1967, **164**, 683.

16 M. E. Lines and A. M. Glass, *Principles and Applications of Ferroelectrics and Related Materials*, Oxford University Press, New York, 1977.

17 (a) A. B. Holder, N. Dalal, R. Fu and R. Migoni, *J. Phys.: Condens. Matter*, 2001, **13**, L231; (b) T. Akutagawa, S. Takeda, T. Hasegawa and T. Nakamura, *J. Am. Chem. Soc*., 2004, **126**, 291.

18 (a) F. Jona and G. Shirane, *Ferroelectric Crystals*, Dover Publications Inc., New York, **1993**; (b) S. Horiuchi, F. Ishii, R. Kumai, Y. Okimoto, H. Tachibana, N. Nagaosa and Y. Tokura, *Nat. Mater.*, 2005, **4**, 163.

Table 1. Crystal structure and refinement detail of **1** at different temperatures.

Temperature (K)	230	200	150	100
Empirical formula	$C_7H_{12}NClF_2O_4$	$C_7H_{12}NClF_2O_4$	$C_7H_{12}NClF_2O_4$	$C_7H_{12}NClF_2O_4$
Formula weight	247.62	247.62	247.62	247.62
Crystal system	Monoclinic	Monoclinic	Monoclinic	Monoclinic
Space group	$P2_1/m$	$P2_1/m$	$P2_1/m$	$P2_1/c$
Unit cell dimensions (Å)	a = 5.8905(3)	a = 5.8745(3)	a = 5.8521(3)	a = 5.8555(5)
	b = 7.5414(5)	b = 7.5347(6)	b = 7.5170(4)	b = 7.4803(6)
	c = 12.7949(7)	c = 12.7728(6)	c =12.7370(6)	c = 24.756(2)
	β = 95.151(5)	β = 94.896(4)	β = 94.458(5)	β = 97.081(8)
V (Å^3)	566.09(6)	563.29(5)	558.61(5)	1076.06(15)
Z, $\rho_{cal.}$ (g/cm^3)	2, 1.453	2, 1.460	2, 1.472	4, 1.529
F(000)	256	256	256	512
Theta range (°)	3.14 - 25.00	3.14 - 25.00	3.15 - 24.99	3.32 - 25.00
Limiting indices	-7<= h <=7	-6<= h <=5	-6<= h <=6	-6<= h <=6
	-8<= k <=8	-7<= k <=8	-8<= k <=8	-8<= k <=8
	-14<= l <=15	-15<= l <=15	-15<= l <=15	-29<= l <=29
Reflections collected / unique	3402 / 1076	2557 / 1070	3501 / 1060	11375 / 1885
	R_{int} = 0.0240	R_{int} = 0.0269	R_{int} = 0.0315	R_{int} = 0.0784
Completeness (%)	99.6	99.6	99.5	99.8
Data/restraints/parameter	1076 / 0 / 90	1070 / 0 / 90	1060 / 0 / 90	1885 / 0 / 139
Goodness	1.072	1.089	1.134	1.104
Final R indices [$I > 2\sigma(I)$]	R_1 = 0.0862	R_1 = 0.0880	R_1 = 0.0874	R_1 = 0.0517
	wR_2 = 0.1699	wR_2 = 0.1707	wR_2 = 0.1571	wR_2 = 0.1070
R indices (all data)	R_1 = 0.1026	R_1 = 0.1042	R_1 = 0.0986	R_1 = 0.0729
	wR_2 = 0.1799	wR_2 = 0.1811	wR_2 = 0.1629	wR_2 = 0.1212

Table of contents (TOC)

Exceptional Dielectric Performance Induced by the Stepwise Reversible Phase Transitions of an Organic Crystal: Betainium Chlorodifluoroacetate

Zhihua Sun, Shuquan Zhang, Chengmin Ji, Tianliang Chen, Junhua Luo

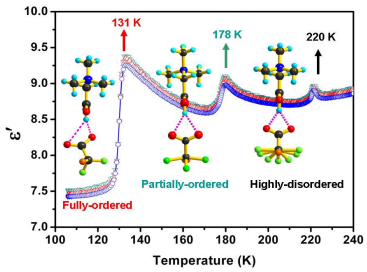

A molecular phase transition material is reported, which exhibits exceptional dielectric performance induced by stepwise structure changes and phase transitions.